Hydrogen transfer in the prphin anion: A quantum dynamical study of vibrational effects

ARTICLE *in* BERICHTE DER BUNSENGESELLSCHAFT/PHYSICAL CHEMISTRY CHEMICAL PHYSICS · MARCH 1998

DOI: 10.1002/bbpc.19981020305

Hydrogen Transfer in the Porphin Anion: A Quantum Dynamical Study of Vibrational Effects

O. Brackhagen*)

Institut für Physikalische und Theoretische Chemie, Freie Universität Berlin, Takustrasse 3, D-14195 Berlin, Germany

Ch. Scheurer and R. Meyer)**

Laboratorium für Physikalische Chemie, Eidgenössische Technische Hochschule, CH-8092 Zürich, Switzerland

H.-H. Limbach

Institut für Organische Chemie, Freie Universität Berlin, Takustrasse 3, D-14195 Berlin, Germany

Key Words: Hydrogen Tunneling / Isotope Effects / Master Equation / Quantum Mechanics

The observed temperature-dependent hydrogen transfer rate constants for the H, D, and T isotopic species of the porphin anion have been reproduced by two different quantum dynamical models. The approach is based on the master equation for the system-state populations. The models involve adapted localization properties and a simplified interaction with a quantum mechanical heat bath. A one-dimensional model describes a hindered circular transfer motion of the hydrogen atom between its four stable sites in the plane of the porphin ring framework. With five parameters that are common to the three isotopic species it yields agreement with the observed data. One of the parameters, the height of the fourfold potential energy barrier, predicts an acceptable estimate for the in-plane N-H wagging frequency. Interactions of the transfer motion with individual vibrations have been studied for a series of two-dimensional model systems. There the circular transfer motion is combined with ring framework modes having properties similar to those obtained for porphin by Li and Zgierski [J. Phys. Chem. *95*, 4268 (1991)]. For vibrational modes near or above 960 cm^{-1}, strong interactions are found to be unlikely, as they would yield kinetic isotope effects and/or apparent activation energies in disagreement with the experimental data. For low frequency modes of the ring framework, however, sizeable couplings with the transfer cannot be ruled out. An interaction of the type suggested by quantum chemical results reported by Vangberg and Ghosh [J. Phys. Chem. B. *101*, 1496 (1997)] has been included in a two-dimensional model involving a rectangular displacement of the pyrrole rings. With low vibrational frequency, a very large coupling strength, and a barrier close to the predicted one, this model has also been found to be compatible with experiment.

1. Introduction

The transfer of hydrogen atoms between stable sites exhibits, due to the small mass of the moving particles, quantum behavior that still needs to be better understood. It also plays a decisive role in biological systems and affects, for instance, the selectivity of enzymatic reactions [1, 2]. For both reasons, hydrogen transfer is intensively studied [3–6] even in large molecular systems [5, 6]. These processes may occur on the whole time scale, from keto-enol tautomerizations in electronically excited states [7], resolved by pump-probe techniques in the femtosecond range [8–10], up to relaxation times in the order of days, as observed by optical spectroscopy in free base porphin at low temperature [11]. Substitution of hydrogen by deuterium or tritium provides a crucial advantage to such studies as it leads to the largest isotope effects known in chemical kinetics. As a unique experimental method, dynamic NMR spectroscopy covers a large time range [12] and allows one to study reactions in thermal equilibrium. Prototype reactions investigated by this method include the simultaneous transfer of two hydrogens in the benzoic acid dimer [13] and the transfer of the two hydrogens in porphin [14]. More recently, the successful synthesis of the conjugate porphin mono-anion [15] and its investigation by NMR [16] have provided experimental data for the interesting case of a single hydrogen atom moving on a potential surface with four minima.

Quantum mechanical descriptions usually involve one or two coordinates to describe the transfer motion and a set of harmonic oscillators representing the environment as a heat bath. The latter includes intramolecular vibrations as well as the lattice modes in condensed phase. Siebrand and coworkers [17–20] emphasize the interaction of the transfer motion with the intramolecular vibrational modes, as obtained from a quantum chemical potential energy surface. Assuming level broadening as a further effect of the environment or using a semiclassical approximation, they calculate the transfer rate constant directly. With this method they have obtained agreement with observations after adjustment of only few parameters. Another approach is concerned with the dynamics of the individual quantum states of the transfer system and assumes a simplified interaction with a continuous set of bath oscillators. Similar to relaxation theory in magnetic resonance [21–23], this yields the master equation for the reduced density matrix [24–28], which is usually restricted to the populations contained in its diagonal part.

*) Present address: Bayer AG, ZF-DID Information und Dokumentation, D-51368 Leverkusen, Germany.
**) Address for correspondence.

  0005-9021/98/0303-0303 $ 17.50+.50/0

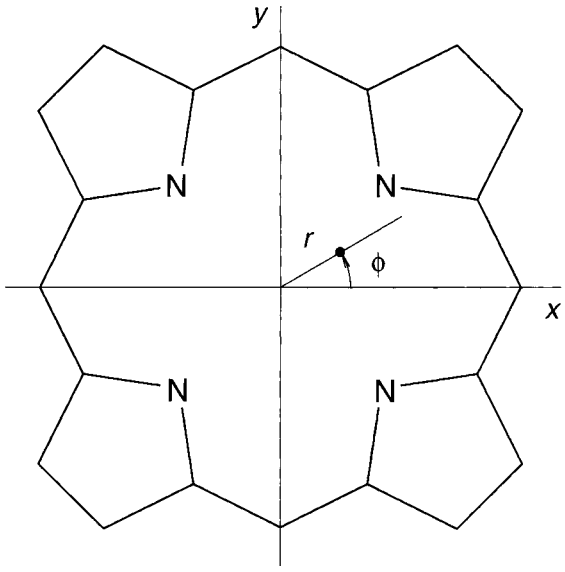

Fig. 1
The planar structure of the porphin anion, carrying a delocalized negative charge, and polar coordinates (r, ϕ) of the hydrogen atom (dot) being transferred between four stable sites. A D_{4h}-symmetric reference structure of the ring framework and equilibrium configurations at $r_e = 1.0$ Å and $\phi_e = \pm 45^\circ, \pm 135^\circ$ are assumed

Tunneling between the two lowest states of a double minimum system has been described by the spin-boson model in a number of investigations reviewed by Leggett et al. [29]. Treatments of this model for the case of a heat bath that includes a single oscillator that is strongly coupled to the system have been proposed by Heuer and Haeberlen [13b] and by Suárez and Silbey [30]. Parris and Silbey [31] have presented the first analytical study on the activation of tunneling by vibrational excitation in a one-dimensional double minimum potential, described by a multilevel system interacting with a bosonic heat bath. A similar model, involving system coordinates for both the transfer motion and for a promoting mode, has been treated [32] in an attempt to understand the experimental hydrogen transfer data of the benzoic acid dimer [13a]. In this treatment, explicit two-dimensional sytem wavefunctions have been obtained numerically [33] and have been used for the evaluation of dynamic properties.

In the present work, we are concerned with the transfer of the single imino hydrogen in the porphin mono-anion. The imino hydrogen atom in this system is able to move from one of the four nitrogen atoms to another in the plane of the porphin ring framework, as shown in Fig. 1. This transfer motion is hindered by barriers in a potential energy function expected to have fourfold periodicity. Braun et al. [16] have found equivalence of the four tautomers within experimental accuracy, observed practically the same kinetic behavior in a solid phase as in a liquid solution, and determined the temperature-dependent hydrogen-transfer rate constants for the protonated (H), deuterated (D) and tritiated species (T). Their analysis of the data in terms of the Arrhenius law has yielded the activation energies $E_a/hc_0 = 1480$, 3600, and 4600 cm^{-1} for the H, D, and T species, respectively. Within the classical picture underlying the Arrhenius law, it is impossible to reproduce these values with an identical energy barrier for all three species. The strong dependence of the apparent activation energies on the isotopic mass is in fact due to tunneling processes, as corroborated in Ref. [16] by the analysis in terms of the modified Bell model and by the present study. Using the approach of Ref. [32], we develop a model containing a set of parameters that are the same in all three isotopic species. Assuming planarity as in the case of porphin [34], the hydrogen atom is allowed to move in the molecular plane between its four stable sites. The general features of such a system, and the conditions for coherent and for incoherent transfer, have been discussed in earlier work [35, 36]. In Sect. 2, we outline the method, referring to a one-dimensional model which, surprisingly, is already found to yield reasonable agreement with experiment. Guided by the normal coordinate work by Li and Zgierski [37] on free base porphin, a variety of hypothetical interactions between the transfer motion and individual vibrational modes of the porphin ring system are investigated in Sect. 3. To assume a strong coupling with a ring system mode at a frequency near and above 960 cm^{-1} turns out to be unrealistic as it leads to apparent activation energies and/or kinetic isotope effects that disagree with observations. On the other hand, sizeable interactions with low frequency vibrations of the ring framework cannot be rule out. In particular, an interaction of the type predicted by Vangberg and Ghosh [38] is found to be compatible with the experimental data.

2. One-Dimensional Model

2.1 Circular Path of Motion

The simplest possible description of the transfer of the hydrogen atom within the plane of the porphin ring framework (see Fig. 1) is obtained by fixing the distance r of the moving particle from the center of this framework at its equilibrium value $r_e = 1.0$ Å, estimated from the heavy atom structure of porphin [34] and from the N-H bond length of pyrrole [39]. The azimuthal angle ϕ then remains as the only variable, and the motion is described by the Hamiltonian

$$H_\phi = -\frac{h^2}{8\pi^2 m r_e^2}\frac{\partial^2}{\partial\phi^2} + V(\phi) \qquad (1)$$

where m is the mass of the hydrogen atom and $V(\phi)$ the potential energy function. On the assumption of a D_{4h} symmetric ring framework, $V(\phi)$ is given as an even fourfold periodic function

$$V(\phi) = B\cos^2 2\phi \qquad (2)$$

involving the barrier height B. The respective time-independent Schrödinger equation is easily solved numerically [33]. The energy levels below the barrier are displayed in

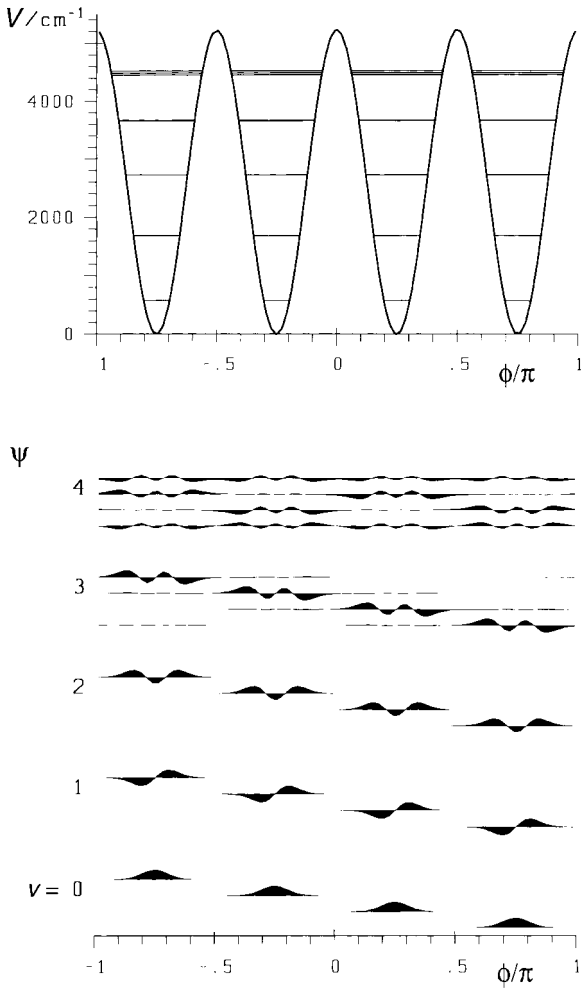

Fig. 2
One-dimensional model for hydrogen transfer in the porphin anion. Potential energy function $V(\phi)$ and energy levels below the barrier. The set of energy levels consists of quartets associated with a given vibrational state of the in-plane N-H wagging vibration. Tunnel splittings become visible on the present scale for the fourth excited vibrational state near the potential energy barrier. The lowest and highest levels in each quartet are nondegenerate and the middle level is twofold degenerate. Diagonalization of a modified Hamiltonian containing an asymmetric perturbation yields the basis functions ψ used in the master equation treatment. They are shown at arbitrary vertical offsets in order to display their localization properties. The localization of these functions is almost complete within quartets with small tunnel splittings but only partial within quartets with large splittings at higher vibrational quantum numbers v. The full set of states used in the dynamical calculations corresponds to that given in Table 1

Fig. 2. The whole set used for the dynamical calculations includes energy levels above the barrier and is listed in Table 1 for each isotopic species. Details on the pattern of eigenstates have been given in Ref. [35]. Tunnel quartets of states with closely spaced levels at energies below the barrier can be labeled by the quantum number $v=0,1,2,...$ of the local vibration in the transfer direction, i.e. of the in-plane N-H wagging mode. By a more general definition that also applies to energy levels above the barrier, $v+1$ is the number of the quartet to which a given energy level belongs (see Table 1). The symmetrized wavefunctions are delocalized and, within a given quartet, similar in magnitude in each of the four potential wells.

2.2 Localized Basis States

When adopting a semiclassical view, the interaction with the environment may be seen as leading to fluctuations in the depths of the potential energy minima of the transfer system. The four minima differ in energy at almost any instant of time by amounts much larger than the tunnel interactions in the lower vibrational states. In the static picture of a snapshot the 'stationary' states are then localized in the minima. In a second snapshot the relative energies of the minima may have changed, possibly even in sign, but the energies are very likely to differ again from one minimum to another. Then the 'stationary' states are still the localized ones although their relative energy has followed the fluctuation of the minima. Hence localization may be expected to survive the fluctuations of the potential energy minima the longer, and to be the more complete, the smaller the tunnel interaction.

To treat the dynamics of the hydrogen transfer by the master equation approach outlined below in Sect. 2.4, we introduce basis states with adaptable localization. They are obtained as linear combinations of wavefunctions that belong to the same vibrational state v. For small tunnel splittings the long-lived localized states are adequate as basis states. At high vibrational excitation, however, where the tunnel splittings increase dramatically and approach the order of magnitude of vibrational spacings (see Table 1), the delocalized eigenstates eventually survive the localized ones and should then be preferred as basis states for the high energy regime. A basis set that exhibits these properties is shown in Fig. 2.

Its construction is heuristic and involves an artificially modified energy matrix whose diagonalization yields the transformation to the basis with adapted localization. The modification of the energy matrix consists of a further contraction of those energy spacings that are already small and of a coupling between eigenstates, which is derived from a symmetry-breaking potential energy term,

$$V_a(\phi) = \Delta V_a[2^{1/2}\sin\phi - (1/2)\sin 2\phi] \; . \qquad (3)$$

The procedure refers to the calculated set of individual energy levels E_i ($i=1,2,...$) ordered by increasing energy. It is controlled by two parameters. One is the factor ΔV_a in Eq. (3), a relatively high threshold to be compared with large tunnel splittings. The other parameter is a low threshold $\Delta E_c>0$. It is used to enhance the sensitivity to an off-diagonal perturbation if an energy gap $\Delta E_i=E_i-E_{i-1}\geq 0$ is below the threshold. The spacing ΔE_i is multiplied by the reduction factor $\Delta E_i/(\Delta E_i+\Delta E_c)$ and will remain practically unchanged if $\Delta E_i \gg \Delta E_c$. But if it is a tunnel splitting near or below ΔE_c, it will be reduced, possibly by orders of magnitude, to the limit $\Delta E_i^2/\Delta E_c$. To obtain the transformation matrix, we first define a modified diagonal matrix with contracted elements

Table 1
Energy levels[a]) of the hydrogen transfer motion in the porphin anion, as calculated for a one-dimensional model for protonated (H), deuterated (D), and tritiated species (T)

Species	v	$\bar{E}_v/hc_0$ [cm^{-1}]	$(E_{v1}-\bar{E}_v)/h$ [MHz]	$(E_{v2}-\bar{E}_v)/h$ [MHz]	$(E_{v3}-\bar{E}_v)/h$ [MHz]	$(E_{v4}-\bar{E}_v)/h$ [MHz]
H	0	0[b])	–5	0	0	5
	1	1113	–300	0	–0	300
	2	2147	–7928	–3	–3	7934
	3	3089	–117482	–655	–655	118791
	4	3913	–967423	–43425	–43425	1054274
	5	4591	–3780783	–528316	–528316	4837416
	6	5247	–8593342	–855289	–855289	10303920
	7	6073	–13182147	–462070	–462070	14106286
D	0	0[b])	0	0	0	0
	1	805	0	0	0	0
	2	1572	–11	0	0	11
	3	2298	–286	0	0	286
	4	2979	–4812	–2	–2	4815
	5	3607	–56163	–206	–206	56575
	6	4170	–433574	–12132	–12132	457839
	7	4645	–1862239	–204903	–204903	2272045
	8	5070	–4568280	–546461	–546461	5661203
	9	5567	–7630462	–354288	–354288	8339037
T	0	0[b])	0	0	0	0
	1	665	0	0	0	0
	2	1305	0	0	0	0
	3	1919	–2	0	0	2
	4	2504	–50	0	0	50
	5	3058	–826	0	0	826
	6	3577	–10168	–8	–8	10185
	7	4055	–92120	–665	–665	93451
	8	4479	–562197	–24748	–24748	611692
	9	4838	–1943734	–242436	–242436	2428607
	10	5179	–4203864	–408768	–408768	5021399
	11	5588	–6350379	–224657	–224657	6799693

[a]) Quartets of states are associated with the quantum number v of the in-plane N-H wagging vibration. $\bar{E}_v$ is the average quartet energy.
[b]) Relative to the potential energy minima, the values are 575 (H), 411 (D), and 338 cm^{-1} (T).

$$E'_1 = E_1 \ ,$$
$$E'_i = E'_{i-1} + \Delta E_i^2/(\Delta E_i + \Delta E_c) \quad (i > 1) \ . \tag{4}$$

Then we add the matrix of the perturbation elements, containing a factor that suppresses any coupling between states belonging to different quartets, which are separated by large energy spacings. The elements of the modified Hamiltonian matrix are thus

$$H'_{ij} = \delta_{ij}[E'_i + \langle i|V_a|i\rangle] + \langle i|V_a|j\rangle \frac{1}{1 + [(E_i - E_j)/\Delta V_a]^8} \tag{5}$$

where the kets $|i\rangle$ and $|j\rangle$ refer to the original wavefunctions ψ_i^0 and ψ_j^0. We are interested in the matrix $\mathbf{U}$ that diagonalizes $\mathbf{H}'$. It yields the basis functions $\psi_\mu = \sum_i \psi_i^0 U_{i\mu}$ with controlled localization, shown in Fig. 2. We distinguish the new representation from the original one by greek indices. Expressed in the new basis $\{|\mu\rangle\}$, the Hamiltonian given by Eqs. (1) and (2) is the sum of a diagonal part H_d and a nonvanishing off-diagonal part ΔH that contains the tunnel interactions:

$$H_\phi = H_d + \Delta H \tag{6}$$

$$H_d = \sum_\mu E_\mu |\mu\rangle\langle\mu| \tag{7}$$

$$\Delta H = \sum_{\mu' \neq \mu} \Delta H_{\mu'\mu} |\mu'\rangle\langle\mu| \ . \tag{8}$$

2.3 Interaction with the Environment

In condensed phase, the system described by the operator $H_\phi = H_d + \Delta H$ interacts with an environment that is thought to be a heat bath consisting of a set of harmonic oscillators. The set includes the vibrations of the ring framework of the particular anion, the intramolecular vibrations of surrounding molecules, and the low frequency lattice vibrations. The interaction is approximated to first order in each bath oscillator coordinate. It is therefore restricted to the in-plane modes of the ring framework and other modes that are parallel to the plane of the ring fra-

mework. We will denote the bath oscillators by their normal coordinates Q but will use the notation q for an individual oscillator 'taken out' of the heat bath. The in-plane vibrations of the porphin anion may be expected to be similar to those of free base porphin which have been investigated by Li and Zgierski [37]. Using their normal coordinates, it is possible to extract the types of interaction with the hydrogen transfer motion. For an individual mode q that oscillates at the frequency ω_q, the interaction term may be given in the general form $f_q\zeta(\phi)q$ where f_q is the interaction force constant and the factor $\zeta(\phi)$ is a 'system coordinate' depending on the symmetry of the mode being described by q. Then the potential energy is, at the point $Q=0$ for all bath oscillators,

$$V(\phi,q) = B\cos^2 2\phi + f_q\zeta(\phi)q + (\omega_q^2/2)q^2 \ . \qquad (9)$$

The arrangement of the four nitrogen atoms, which is approximately a square at equilibrium, is deformed in many of the normal coordinates. This deformation may serve to determine the dependence of the respective system factor ζ on the transfer coordinate ϕ. A number of modes of species a_g with respect to D_{2h} symmetry, see Ref. [37], involve a rhombic deformation, as shown in Fig. 3a. By this deformation the equivalence of neighboring stable hydrogen sites is lifted but it is preserved for sites that are opposite to each other. According to Eq. (9) this behavior is obtained with $\zeta(\phi)=\sin 2\phi$. At $\phi=\pi/4$ we have $\zeta=1$ and $V(\pi/4,q)=f_q\,q+(\omega_q^2/2)q^2$. This function reaches a minimum at $q_e=-f_q/\omega_q^2$, where it is lowered, relative to the point $q=0$, by the "individual rearrangement energy" $\Delta V_{Rq}=V(\pi/4,0)-V(\pi/4,q_e)$ given by

$$\Delta V_{Rq} = (1/2)f_q^2/\omega_q^2 \ . \qquad (10)$$

This behavior is illustrated by the potential energy surface $V(\phi,q)$ shown in Fig. 3a. Similarly, the rectangular deformations, contained in b_{1g} modes of porphin [37], are found to be associated with the system factor $\zeta(\phi)=\cos 2\phi$. In this case the saddle points of the potential energy surface, rather than the minima, are shifted along the q direction and are lowered, relative to the value at $q=0$, by the same amount ΔV_{Rq}, see Fig. 3b. If q describes a trapezoidal deformation such as the one shown in Fig. 3c, its coupling to the transfer motion involves the factor $\zeta(\phi)=\sin\phi$. This causes pairs of neighboring saddle points to move in opposite directions along q and to be lowered by the amount ΔV_{Rq} relative to the value at $q=0$. The minima are shifted towards the closest one of the displaced saddle points and are lowered approximately by the amount $2^{-1/2}\Delta V_{Rq}$ for $\Delta V_{Rq}\ll B$. When rotating the trapezoid shown in Fig. 3c clockwise by $\pi/2$, it represents a deformation due to another coordinate that oscillates, in the limit of a D_{4h} symmetric framework, at the same frequency as the previous one. The new coordinate is associated with $\zeta(\phi)=\cos\phi$ and forms a degenerate pair with the one coupled by the factor $\zeta(\phi)=\sin\phi$. In phase and out of phase combinations of the two describe the kite-shaped deformations that appear as components of b_{2u} and b_{3u} modes in porphin [37]. The in-plane modes can be classified by their transformation properties with respect

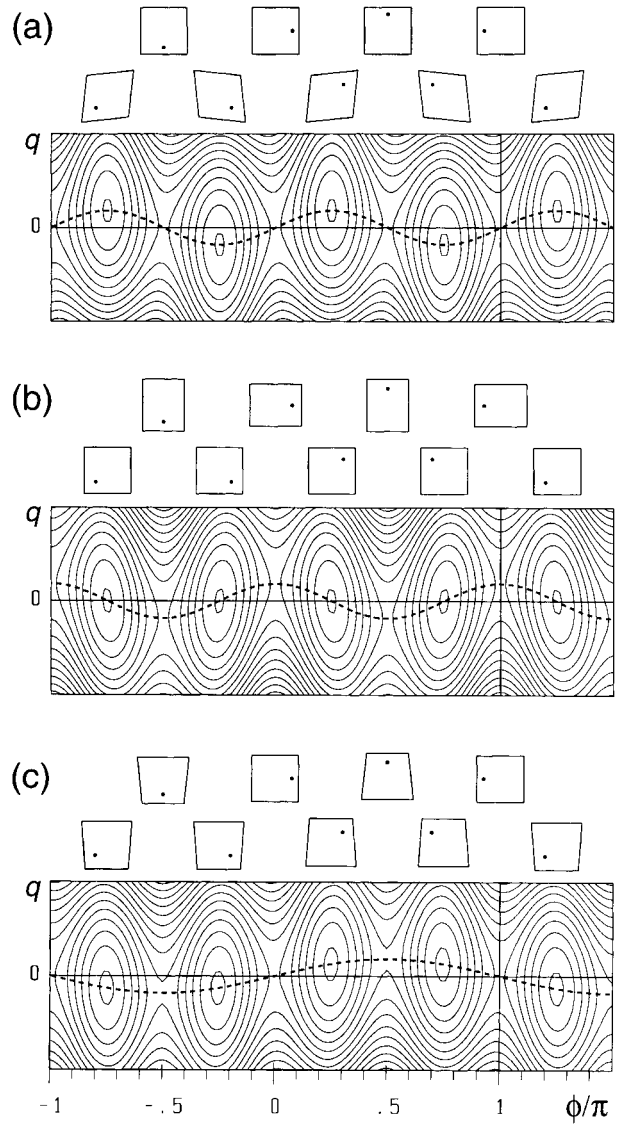

Fig. 3
Interaction of the hydrogen transfer motion (ϕ) with individual in-plane vibrational coordinates (q) of the ring framework in the porphin anion. The vibrational coordinates are characterized by distortions of the arrangement of the four nitrogen atoms from a square at $q=0$ to quadrilaterals at $q\neq 0$. With the dot indicating the position of the imino hydrogen atom, schematic configurations are shown for the potential energy minima (lower rows) and saddle points (upper rows). The potential energy functions $V(\phi,q)$ involve coupling terms $f_q\zeta(\phi)q$ with force constants f_q leading to a common individual rearrangement energy $\Delta V_{Rq}/hc_0=200\ \mathrm{cm}^{-1}$. Contours are shown at $V/hc_0=100,\ 1100,\ 2100,\ldots\ \mathrm{cm}^{-1}$. The minimum energy paths (dashed curves) correspond to the coupling factors $\zeta(\phi)$ and involve displacements of the potential minima (ϕ_e, q_e) and/or saddle points $(\phi^{\ddagger}, q^{\ddagger})$ along the q direction. (a) Rhombic distortions, $\zeta=\sin 2\phi$, $\Delta V_{Rq}=V(\phi_e,0)-V(\phi_e,q_e)$. (b) Rectangular distortions, $\zeta=\cos 2\phi$, $\Delta V_{Rq}=V(\phi^{\ddagger},0)-V(\phi^{\ddagger},q^{\ddagger})$. (c) Trapezoidal distortions, $\zeta=\sin\phi$, $\Delta V_{Rq}=V(\pm\pi/2,0)-V(\pm\pi/2,\ q^{\ddagger})$. Similar to the latter case, a symmetrically equivalent fourth potential energy surface is obtained with $\zeta=\cos\phi$

to the group C_{4v}. Then the modes q_c and q_s and the respective system coupling factors $\cos\phi$ and $\sin\phi$ belong to the species E. Similarly a mode q_{c2} and the associated factor $\cos 2\phi$ belong to the species B_1 and a mode q_{s2} as well as the corresponding factor $\sin 2\phi$ belong to the species B_2.

A similar structure as for the set of framework modes is assumed for the entire heat bath whose Hamiltonian H_Q is thought to consist of many terms $(1/2)[P^2+\omega^2Q^2]$ referring to oscillations parallel to the plane of the ring system. Its coupling with the transfer system is contained in the overall potential energy function and is approximated to first order with respect to the bath coordinates and to second order with respect to the hydrogen coordinates $x=r\cos\phi$, $y=r\sin\phi$, which are restrictred, however, by the condition that x^2+y^2 must remain constant. Nonzero coupling terms must be totally symmetric with respect to the group C_{4v}, that is, they are again of the types $\cos\phi\, Q_{c,i}$, $\sin\phi\, Q_{s,i}$, $\cos 2\phi\, Q_{c2,i}$, $\sin 2\phi\, Q_{s2,i}$ and involve symmetry-adapted linear combinations of bath oscillator displacements. Within our simplified model of the heat bath we assume symmetry-adapted bath coordinates $Q_{c,i}$, $Q_{s,i}$, $Q_{c2,i}$, and $Q_{s2,i}$ and neglect the coupling between the different species. This is a further approximation since a general bath coordinate is asymmetric. The total Hamiltonian is then given as

$$H_{\text{total}} = H_\phi I_Q + H_{\phi Q} + I_\phi H_Q \tag{11}$$

where I_Q and I_ϕ are the identity operators acting on the space of bath states and on the space of transfer-system states, respectively, while H_Q and $H_{\phi Q}$ refer to the four subsets of symmetry-adapted bath oscillators,

$$H_Q = H_{Qc} + H_{Qs} + H_{Qc2} + H_{Qs2}\ , \tag{12}$$

$$H_{\phi Q} = \cos\phi \sum_i f_{c,i} Q_{c,i} + \sin\phi \sum_i f_{s,i} Q_{s,i} + \cos 2\phi \sum_i f_{c2,i} Q_{c2,i} + \sin 2\phi \sum_i f_{s2,i} Q_{s2,i}\ . \tag{13}$$

The effect of a given bath mode on the transfer motion depends on its frequency ω, on the associated coupling factor $\zeta(\phi)$, and on the magnitude of the coupling force constant f that is related to the individual rearrangement energy $(1/2)f^2/\omega^2$. Assuming a continuum of bath oscillators, we obtain a spectral distribution of individual rearrangement energies, involving the density of modes $\rho(\omega)$. Since little is known about this distribution, a model assumption [32] is made,

$$(1/2)\rho(\omega)[f(\omega)/\omega]^2 = (2^{3/2}/\pi)\Delta V_R \omega_p \frac{\omega^2}{\omega_p^4+\omega^4}\ . \tag{14}$$

The distribution contains the parameters ω_p and ΔV_R. It has a peak at the frequency ω_p, and its integral over the range $(0\le\omega\le\infty)$ equals ΔV_R, the overall rearrangement energy of the bath. We apply Eq. (14) with the same parameters to each of the four parts distinguished in Eqs. (12) and (13).

2.4 Rate Processes

The dynamics of the transfer system is expected to correspond to the incoherent limit [35] and to be describable, in an adequately localized basis, by a master equation restricted to the populations. For the populations p_μ of the states constructed in Sect. 2.2, this equation can be written as

$$\mathrm{d}p_{\mu'}/\mathrm{d}t = \sum_\mu W_{\mu'\mu} p_\mu\ . \tag{15}$$

It describes the relaxation to thermal equilibrium in terms of temperature-dependent probabilities per unit time $W_{\mu'\mu}$ for the transitions $\mu'\leftarrow\mu$, analogous to the rate constants in a first order chemical kinetic system. In the present form of the master equation, the **W**-matrix must have the diagonal elements $W_{\mu\mu}=-\sum_{\mu'\neq\mu} W_{\mu'\mu}$, as required by the mass conservation law. The transition probabilities are obtained from a time-dependent second order perturbation treatment as elaborated in Ref. [32] for a system with a single system-bath interaction factor ζ. It uses a numerical representation of the basis functions $\psi_\mu(\phi)$, the distribution function in Eq. (14), and the values of the matrix elements in Eqs. (7) and (8). Each transition probability consists, in general, of both "tunneling" and "vibrational" contributions, depending on the elements $\Delta H_{\mu'\mu}$ and $\zeta_{\mu'\mu}=\langle\mu'|\zeta(\phi)|\mu\rangle$, respectively,

$$W^{\text{tun}}_{\mu'\mu} \propto [\Delta H_{\mu'\mu}]^2 \tag{16}$$

and

$$W^{\text{vib}}_{\mu'\mu} \propto [(\cos\phi)_{\mu'\mu}]^2 + [(\sin\phi)_{\mu'\mu}]^2 + [(\cos 2\phi)_{\mu'\mu}]^2 + [(\sin 2\phi)_{\mu'\mu}]^2\ . \tag{17}$$

For localized states $|\mu'\rangle$ and $|\mu\rangle$, the total transition probability

$$W_{\mu'\mu} = W^{\text{tun}}_{\mu'\mu} + W^{\text{vib}}_{\mu'\mu} \tag{18}$$

is dominated by $W^{\text{tun}}_{\mu'\mu}$ if the two states are associated with the same state (v) of local vibration and by $W^{\text{vib}}_{\mu'\mu}$ otherwise. Details of the calculation for the present case of four different interaction factors $\zeta(\phi)$ are summarized in the Appendix. With a known **W**-matrix, Eq. (15) can be integrated to yield a detailed description of the population transfer among the system states,

$$p_{\mu'}(t) = \sum_\mu (\mathrm{e}^{Wt})_{\mu'\mu} p_\mu(0)\ , \tag{19}$$

that has been exploited, for instance, by Scheurer and Saalfrank [40]. In the long run, the populations approach the Boltzmann equilibrium, $p_{\mu'}(t\to\infty)=p^0_{\mu'}$, for any set of initial populations $p_\mu(0)$.

In order to define the hydrogen transfer rate constant, we consider the hydrogen delocalization as an overall process monitored by the correlation decay of a localized probing function,

$$Z(\phi) = [1 - 2^{1/2}(\cos\phi + \sin\phi) + \sin 2\phi] \,, \tag{20}$$

using the method due to Look and Lowe [41] as applied in Ref. [13a]. It is based on the time-dependent expectation value $\langle Z\rangle_t = \sum_{\mu'} Z_{\mu'\mu'} p_{\mu'}(t)$ where $Z_{\mu'\mu'} = \langle\mu'|Z(\phi)|\mu'\rangle$. If only a single state μ is populated initially, the expectation value at $t=0$ is $\langle Z\rangle_0^{(\mu)} = Z_{\mu\mu}$ and becomes $\langle Z\rangle_t^{(\mu)} = \sum_{\mu'} Z_{\mu'\mu'}(\mathrm{e}^{Wt})_{\mu'\mu}$ at $t>0$, according to Eq. (19). At thermal equilibrium the chosen initial condition has a probability given by the Boltzmann weight p_μ^0 and hence contributes the term $\langle Z\rangle_t^{(\mu)}\langle Z\rangle_0^{(\mu)} p_\mu^0$ to the correlation function

$$C_{ZZ}(t) = \sum_{\mu'\mu} Z_{\mu'\mu'}(\mathrm{e}^{Wt})_{\mu'\mu} Z_{\mu\mu} p_\mu^0 \,. \tag{21}$$

Initially at $C_{ZZ}(0) = \sum_\mu (Z^2)_{\mu\mu} p_\mu^0$, this function decays to $C_{ZZ}(\infty) = (\sum_\mu Z_{\mu\mu} p_\mu^0)^2$. Its relaxation time is defined by

$$\tau_c = \int_0^\infty \mathrm{d}t \frac{C_{ZZ}(t) - C_{ZZ}(\infty)}{C_{ZZ}(0) - C_{ZZ}(\infty)} \tag{22}$$

and yields the correlation decay rate constant as our measure for the hydrogen transfer rate constant,

$$k = 1/\tau_c \,. \tag{23}$$

The numerical evaluation of Eqs. (19), (21) and (22) has been described earlier [13a].

2.5 Results

The one-dimensional model described above has been fitted to the observed data reported by Braun et al. [16] and has yielded the results shown in Fig. 4. The standard deviation of the natural logarithm of the rate constants is $\sigma(\ln k) = 0.12$ and corresponds to an approximate error of 12% in k, probably not much larger than the experimental uncertainty. The model parameters are given in Table 2.

The barrier obtained from the fit, $B/hc_0 = 5220.7\ \mathrm{cm}^{-1}$, is the one used to calculate the energy levels given in Table 1 and corresponds to that shown in Fig. 2. It places the fundamental in-plane N-H and N-D wagging frequencies at 1113 and 805 cm^{-1}, respectively (see Table 1). In the porphin species with two imino H atoms, this motion is contained [37] in modes at 1226 (b_{1g}) and 1223 cm^{-1} (b_{2u}), shifted upwards by interaction with framework deformations that dominate the modes at 976 (b_{1g}) and 986 cm^{-1} (b_{2u}). The interaction effect is less pronounced in the species with two imino D atoms, where the calculated modes dominated by the in-plane N-D wagging motions oscillate at 818 (b_{1g}) and 825 cm^{-1} (b_{2u}), rather similar to the predicted frequency of 805 cm^{-1} for the D species of the porphin anion. Apparently, the barrier is not only consistent with the kinetic data of the hydrogen transfer motion but also gives a reasonable estimate for its vibrational fundamental frequency.

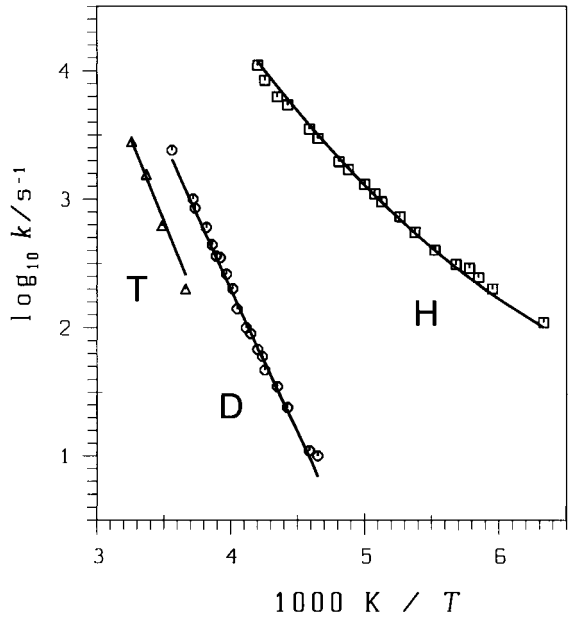

Fig. 4
Temperature dependence of the hydrogen transfer relaxation rate constant in the porphin anion. Squares, circles, and triangles indicate experimental data from Ref. [16] for H, D, and T species, respectively. The lines show the results calculated for a one-dimensional model

Table 2
Parameters of a one-dimensional model for hydrogen transfer in the porphin anion

Parameter	Units	Value
B/hc_0	cm^{-1}	5220.7 (30)[a]
$\omega_p/2\pi c_0$	cm^{-1}	30.4 (18)
$\Delta V_R/hc_0$	cm^{-1}	46.9 (26)
$\Delta V_a/hc_0$	cm^{-1}	24.6 (11)
$\Delta E_c/h$	MHz	105 (28)

[a]) Numbers in parentheses give standard deviations in units of last digit.

The individual rearrangement-energy distribution, Eq. (14), that measures the system-bath interaction strength as a function of bath-mode frequency, has its peak at $\omega_p/2\pi c_0 = 30.4\ \mathrm{cm}^{-1}$, which is relatively low and hence indicates a predominant effect of lattice phonons of the condensed environment. As given by the overall rearrangement energy $\Delta V_R/hc_0 = 46.9\ \mathrm{cm}^{-1}$ for each of the four subsets of bath modes distinguished in Sect. 2.3, the total interaction strength appears to be sufficiently small to justify the perturbation approach applied.

Even if the parameters ΔV_a and ΔE_c are linked to the particular scheme of localization given in Sect. 2.2, rather than directly representing physical quantities, they contain physical information. Within a given tunneling quartet,

the localization is only marginal if the level separations are much larger than the upper threshold $\Delta V_a/hc_0 = 24.6\ cm^{-1}$ (737 GHz) but it becomes the more significant the smaller the absolute splittings are relative to this threshold. The localization is practically complete if the splittings are much smaller than the lower threshold, $\Delta E_c = 105$ MHz. Localization properties based on these parameters are illustrated in Fig. 2. By considering the splittings listed in Table 1, significant localization is found only for the states associated with vibrational quantum numbers up to $v=3$ for the H species, up to $v=6$ for the D species, and up to $v=8$ for the T species, while higher energy states of the respective species remain delocalized. Similarly, the localization is found to be (almost) complete for the four $v=0$ states of the H species, for the states associated with $v=0$, 1, and 2 in the case of the D species, and for those associated with $v=0$, 1, 2, 3, and 4 for the T species.

A considerable sensitivity of the results to the extent of localization of the basis functions was found in preliminary calculations. Imposing the restriction $\Delta E_c = \Delta V_a$ led to a standard deviation $\sigma(\ln k) = 0.16$ with fitted parameters (in cm^{-1}) $B/hc_0 = 5130$, $\omega_p/2\pi c_0 = 40$, $\Delta V_R/hc_0 = 7.7$, $\Delta V_a/hc_0 = 2.0$. The corresponding $\ln k$ vs. $1/T$ diagram for the H species exhibited a significantly exaggerated curvature, and this feature persisted many tentative modifications of the model. The modifications included a second term $B'\sin^2 4\phi$ in the potential energy function with the additional parameter B', a non-circular path of motion described by $r(\phi) = r_e + \Delta r \cos^2 2\phi$ with the new parameter Δr, a second peak in the individual rearrangement-energy distribution with additional parameters, and the extension to rearrangement-energy distributions differing for the coupling factors $\cos 2\phi$ and/or $\sin 2\phi$ from that for $\cos\phi$ and $\sin\phi$. All of these modifications, and all of the extensions to two-dimensional models discussed in the following section, failed to reduce the exaggerated curvature in $\ln k$ vs. $1/T$ for the H species, as long as the restriction $\Delta E_c = \Delta V_a$ was maintained. We are therefore quite convinced that the two independent parameters ΔV_a and ΔE_c describe, although in a heuristic manner, physically relevant localization properties.

The activation of the hydrogen transfer is related to the population of excited states with increasing temperature [32]. It depends on the growth of the tunnel splittings in absolute value upon progressive excitation (see Table 1) and therefore behaves differently in the H, D, and T species. The fit of the data by the one-dimensional model implies that in the experimental temperature range the hydrogen transfer appears as 'self promoting', which means that there is virtually no promotion of the transfer by any mode other than the hydrogen-atom vibration in the transfer direction itself.

3. Strong Coupling with Individual Vibrations

While the fit of a one-dimensional model to the experimental data has been successful, this outcome may not in itself be sufficient to prove the absence of major interactions between the hydrogen transfer motion and individual modes of the ring framework. In order to study this question, and the possibility of promotion by a mode other than the N-H wagging, we investigate the effects of such interactions even if they may be hypothetical. The calculated interaction effects for nine different models are shown in Table 3.

3.1 Common Properties and Procedures

In free base porphin, framework modes cluster around 1600 and 960 cm^{-1} in the mid-infrared frequency range, and near or below 300 cm^{-1} [37]. We therefore consider a number of modes at or near these frequencies, incorporated, one at a time, in a two-dimensional system Hamiltonian

$$H_{\phi q} = -\frac{h^2}{8\pi^2 m r_e^2}\frac{\partial^2}{\partial\phi^2} - \frac{h^2}{8\pi^2}\frac{\partial^2}{\partial q^2} + V(\phi, q) \qquad (24)$$

where the potential energy function $V(\phi,q)$ is given as in Eq. (9). We retain the parameters as obtained for the one-dimensional model and make an assumption on the individual rearrangement energy of the q mode, Eq. (10). The direct calculation [33] of the energy levels E_i and wavefunctions $\psi_i^0(\phi,q)$ is easy to apply if the frequency ω_q is similar to or higher than that of the N-H wagging mode but is rendered awkward by the sheer number of states needed if the framework mode is at low frequency. In this case, however, an adiabatic approximation is adequate.

As in the one-dimensional model, the representation of $H_{\phi q}$ in a localized basis $\{\psi_\mu(\phi,q)\}$ obtained by the procedure of Sect. 2.2 leads to a decomposition into diagonal and off-diagonal parts given by Eqs. (7) and (8), respectively. In the total Hamiltonian, obtained from Eq. (11) after changing the subscript ϕ to ϕq, the environment part is again decomposed as in Eq. (12). The interaction part $H_{\phi qQ}$ is assumed to be the same as in Eq. (13), except for a fifth term, $\zeta_q \sum_i f_{\gamma,i} Q_{\gamma,i}$, that is added in the case of the direct calculation for a framework mode q at or above 960 cm^{-1}. The q mode may be coupled by such a term to the bath modes of its own symmetry species γ and is then allowed to relax independently of the transfer motion. The force constants $f_{\gamma,i}$ are again related to the common distribution of individual rearrangement energies (Eq. (14)). The coordinate value q_{tp} at the turning point in the ground state of the q vibration and a factor a are used to define the system interaction factor as $\zeta_q = aq/q_{tp}$. However, as the results have been found to be rather insensitive to the extra term for $0 \le a \le 2$, we choose $a=1$. The calculations leading to the transition probabilities and to the rate constants remain the same as those described above in Sect. 2.4. Exceptions are the expressions for the transition probabilities obtained from the adiabatic approximation for the low-frequency modes in models 3, 6, and 9 as described below.

Table 3
Coupling effects of individual vibrations on hydrogen transfer in the porphin anion

Model[a])	$\zeta(\phi)$	ν_q/c_0 [cm^{-1}]	$\Delta V_{Rq}/hc_0$ [cm^{-1}]		T/K					
					158	181	215	238	273	307
1	sin2ϕ	1600	200	$\Delta\ln k_H$[b])	–0.31	–0.23	–0.17	–0.14		
				$\Delta\ln k_D$			–0.12	–0.05	–0.01	
				$\Delta\ln k_T$					0.02	0.05
2	sin2ϕ	960	100	$\Delta\ln k_H$	–0.31	–0.22	–0.13	–0.05		
				$\Delta\ln k_D$			–0.14	–0.06	–0.02	
				$\Delta\ln k_T$					0.34	0.48
3[c])	sin2ϕ	157	10	$\Delta\ln k_H$	–0.33	–0.36	–0.37	–0.36		
				$\Delta\ln k_D$			–0.25	–0.26	–0.25	
				$\Delta\ln k_T$					–0.20	–0.19
4	cos2ϕ	1600	200	$\Delta\ln k_H$	–0.02	–0.02	0.02	0.06		
				$\Delta\ln k_D$			0.14	0.36	0.21	
				$\Delta\ln k_T$					0.27	0.34
5	cos2ϕ	1050	200	$\Delta\ln k_H$	–0.66	–0.84	–0.71	–0.52		
				$\Delta\ln k_D$			0.19	0.25	0.36	
				$\Delta\ln k_T$					0.82	0.91
6[c])	cos2ϕ	109	200	$\Delta\ln k_H$	–0.70	–0.81	–0.80	–0.75		
				$\Delta\ln k_D$			–1.00	–0.92	–0.81	
				$\Delta\ln k_T$					–0.83	–0.73
7	sinϕ	1600	140	$\Delta\ln k_H$	–0.14	–0.15	–0.10	–0.06		
				$\Delta\ln k_D$			0.04	0.00	0.02	
				$\Delta\ln k_T$					0.03	0.03
8	sinϕ	960	140	$\Delta\ln k_H$	–0.35	–0.42	–0.39	–0.28		
				$\Delta\ln k_D$			–0.01	0.06	0.08	
				$\Delta\ln k_T$					0.20	0.24
9[d])		340	70	$\Delta\ln k_H$	–0.45	–0.45	–0.46	–0.45		
				$\Delta\ln k_D$			–0.38	–0.42	–0.41	
				$\Delta\ln k_T$					–0.38	–0.37

[a]) q is the coordinate of a harmonic mode at frequency $\omega_q = 2\pi\nu_q$, coupled to the transfer coordinate ϕ by the term $\zeta(\phi)\ \omega_q\ (2\Delta V_{Rq})^{1/2} q$.
[b]) $\ln k$ is the natural logarithm of the hydrogen transfer relaxation rate constant, $\Delta\ln k$ is the change relative the one-dimensional model value, as calculated for H, D and T species.
[c]) Results from adiabatic approximation.
[d]) Results from adiabatic approximation for two degenerate vibrations q_c and q_s with coupling term $(\cos\phi\ q_c + \sin\phi\ q_s)\ \omega_q\ (2\Delta V_{Rq})^{1/2}$.

3.2 Modes Coupled by sin 2ϕ

Taking the simpler cases first, as outlined in Fig. 3, we choose a coordinate q that is coupled to the transfer motion by the factor $\zeta(\phi) = \sin 2\phi$. Porphin modes of this type are, for instance, ν_{10} at 1611, ν_{12} at 1353, ν_8 at 971, ν_{15} at 956, and ν_{18} at 157 cm^{-1} [37]. We will assume the frequencies 1600, 960, and 157 cm^{-1} in models 1, 2, and 3, respectively. On the potential energy surface given by Eq. (9), the profile along the minimum energy path has the same shape as in the one-dimensional model but extends from $-\Delta V_{Rq}$ at the minima to B at the saddle points, resulting in a higher barrier, $B+\Delta V_{Rq}$. In order to recover the original barrier height, we add the term $\Delta V_{Rq}\sin^2 2\phi$. With ΔV_{Rq} related by Eq. (10) to the coupling force constant f_q and the frequency ω_q we obtain the potential surface which is used in models 1–3 and shown in Fig. 3 a,

$$V(\phi, q) = B\cos^2 2\phi + (\omega_q^2/2)[q + \sin 2\phi f_q/\omega_q^2]^2 \ . \quad (25)$$

An adiabatic approximation is used for model 3 that includes the mode at 157 cm^{-1}. The basis functions are products $\psi_\mu(\phi)\chi_{\mu\nu}(q)$. The factors $\psi_\mu(\phi)$ of the transfer subsystem H_ϕ are obtained as described in Sect. 2.2 with elements E_μ and $\Delta H_{\mu'\mu}$ given by Eqs. (7) and (8), respectively, and with system-bath coupling elements calculated as $\zeta_{\mu'\mu} = \langle\mu'|\zeta(\phi)|\mu\rangle$ for all four coupling factors. The vibrational factors $\chi_{\mu\nu}(q)$ are harmonic oscillator eigenfunctions associated with the energy levels E_ν. They depend on μ as a parameter, $\chi_{\mu\nu}(q) = \chi_\nu(q - q_{0\mu})$, by a shift in origin,

$$q_{0\mu} = -(\sin 2\phi)_{\mu\mu} f_q/\omega_q^2 \ , \quad (26)$$

as may be expected for localized wavefunctions on the potential energy surface shown in Fig. 3 a. Since the

($\Delta v \neq 0$, $\Delta\mu = 0$) transitions are probably very fast and the ($\Delta v \neq 0$, $\Delta\mu \neq 0$) transition negligibly slow [32], we assume thermal equilibrium for the q mode and calculate the average probabilities of ($\Delta v = 0$, $\Delta\mu \neq 0$) transitions. With respect to the product state basis $\{\psi_\mu \chi_{\mu v}\}$ we replace, for instance, the element $\Delta H_{\mu'\mu} = \langle \mu' | \Delta H | \mu \rangle$ in Eq. (16) by $\langle \chi_{\mu' v} | \langle \mu' | \Delta H | \mu \rangle | \chi_{\mu v} \rangle$, multiply the squared element by the Boltzmann population p_v^0 of the vibrational level E_v, sum over v and find

$$W_{\mu'\mu}^{\text{tun}} \propto [\Delta H_{\mu'\mu}]^2 \sum_v p_v^0 \langle \chi_{\mu' v} | \chi_{\mu v} \rangle^2 \,. \tag{27}$$

Using a numerical representation of the harmonic oscillator wavefunctions on a grid, we calculate the overlap integrals $\langle \chi_{\mu' v} | \chi_{\mu v} \rangle$ of functions with different centers, Eq. (26), to evaluate the sum in Eq. (27). The sum represents the mean square vibrational overlap. It appears as a factor also in the analogous expression for $W_{\mu'\mu}^{\text{vib}}$ and for the total transition probability $W_{\mu'\mu}$.

Model 1. The q mode at 1600 cm^{-1}, coupled to the transfer motion with a strength given by the rearrangement energy 200 cm^{-1}, causes in the H species a slow-down of the transfer that levels off with increasing temperature (see Table 3). The effect may be attributed to the fact that q must change upon going from one minimum to another (see Fig. 3). This implies a heavier effective mass being transferred and hence results in a slower tunneling motion. In a vibrationally excited state of the q mode, a wider range of q values is accessible and in part of this range the hydrogen may tunnel without further q displacement, that is, with its own lighter mass. In the excited state of the q mode, the tunnel interaction is therefore enhanced and its thermal population may thus explain the moderation of the slow-down at higher temperature. A similar slow-down obtained for the D species is smaller, on a relative scale, because of a smaller relative change in effective mass. A slight promotion of the transfer, increasing with temperature, is found in the T species as a result of thermally accessible states with larger tunnel interactions that are not available without the coupling to the q mode.

Model 2. When lowering the q-mode frequency to 960 cm^{-1} and, simultaneously, the rearrangement energy to 100 cm^{-1}, the behavior of the H and D species remains practically the same as in model 1. However, the promotion in the T species is markedly enhanced, due to facilitated population of the lower lying excited vibrational states of the q mode. The tunnel interactions in these states are enhanced relative to those in excited N-T wagging states and allow the q mode to compete with the N-T wagging mode in promoting the transfer.

Model 3. With a frequency as low as 157 cm^{-1}, a rearrangement energy of 10 cm^{-1} is sufficient to produce a similar slow-down at 158 K in the H species as in models 1 and 2. Here the effect changes little with temperature and with isotopic mass, indicating a predominant increase in effective mass (or a reduced vibrational overlap) in all three species. Due to the low frequency, excitation of the q mode is expected to activate the transfer process only below the experimental temperature range.

3.3 Modes Coupled by cos2ϕ

Examples for porphin ring framework modes coupled to the transfer motion by the factor $\zeta(\phi) = \cos 2\phi$ are ν_{19} at 1600, ν_{28} at 1493, ν_{22} at 976, and ν_{35} at 109 cm^{-1} [37]. In our models 4–6, we adopt the frequencies 1600, 1050, and 109 cm^{-1}, and a common rearrangement energy of 200 cm^{-1}. Again a potential energy function as given by Eq. (25) after replacing sin2ϕ by cos2ϕ is used for models 4–6 and shown in Fig. 3b,

$$V(\phi, q) = B \cos^2 2\phi + (\omega_q^2/2)[q + \cos 2\phi f_q/\omega_q^2]^2 \,. \tag{28}$$

On this surface, the saddle points are of the same height B as in the one-dimensional model but can be reached only when displacing the q coordinate.

The adiabatic approximation used in the case of model 6 with the mode at 109 cm^{-1} differs from that of the previous section, since here the shifts of the wavefunctions along q are zero by symmetry (see Fig. 3b) while the tunnel interactions are strongly dependent on q. Treating this variable as a parameter in the ϕ-dependent part of the Hamiltonian, Eq. (24), we calculate the energy levels as functions $E_i(q)$ and find negligible dependence on q if compared with the oscillator potential function $(\omega_q^2/2)q^2$, but the relative change in the splittings within a narrowly spaced quartet is large. The states are ordered by correspondence of wavefunctions ψ_i^0. Then the two functions $E_\pm(q)$ that correspond to degenerate levels at $q = 0$ are related by $E_+(q) = E_-(-q)$. In the product basis $\{\psi_\mu \chi_\nu\}$, the transfer-system factors $\psi_\mu = \sum_i \psi_i^0 U_{i\mu}$ are constructed, as described in Sect. 2.2, from the solutions E_i, ψ_i^0 obtained for $q = 0$. The transformation is then applied to the diagonal matrix containing the q-dependent energy levels $E_i(q)$ and yields q-dependent matrix elements $E_\mu(q)$ and $\Delta H_{\mu'\mu}(q)$ as successors to those in Eqs. (7) and (8), respectively. The vibrational factors $\chi_\nu(q)$ are again represented numerically on a grid in order to calculate the elements $\langle v | E_\mu(q) | v \rangle$ that are almost independent of v. As in Sect. 3.2, we assume thermal equilibrium of the q mode and calculate the average probabilities of the ($\Delta v = 0$, $\Delta\mu \neq 0$) transitions. The tunneling contribution

$$W_{\mu'\mu}^{\text{tun}} \propto \sum_v p_v^0 \langle v | \Delta H_{\mu'\mu}(q) | v \rangle^2 \,. \tag{29}$$

is now proportional to a temperature-dependent mean square tunnel interaction, whereas the vibrational contribution remains as given by Eq. (17).

Model 4. The interaction effects shown in Table 3 for this model, with a q mode at 1600 cm^{-1}, indicate a marginal slow-down of the transfer in the H species at the lower two temperatures. This may be attributed to the higher barrier in the ground state of the q mode that restricts the configurations to the vicinity of $q=0$ (see Fig. 3b). Excitation of the q mode allows the system to move closer to the saddle points and may explain the weak acceleration obtained at the two higher temperatures. In the D and T species, the latter effect is stronger, on a relative scale, and dominant.

Model 5. This model mimics the behavior of the b_{1g} modes ν_{22} and δ_{NH} in porphin whose crossing upon deuteration has been investigated in Ref. [37]. We assume the q-mode frequency at 1050 cm^{-1}, near the uncoupled in-plane N-H wagging fundamental at 1113 cm^{-1} (see Table 1). The direct calculation of the states E_i, $\psi_i^0(\phi, q)$ yields the shifted fundamentals at 970 and 1204 cm^{-1} for the H species and at 1077 and 784 cm^{-1} for the D species. From the similarity of this pattern to that for ν_{22} and δ_{NH} in porphin the coupling strength given by $\Delta V_{Rq}=200$ cm^{-1} appears to be realistic. The considerable slow-down obtained with this model for the hydrogen transfer in the H species (see Table 3) is explained by the sharing of the 300 MHz splitting in the uncoupled first excited state (see Table 1) among the two first excited states in the coupled system. As the splitting of the state at 970 cm^{-1} is close to 100 MHz and that of the state at 1204 cm^{-1} close to 200 MHz, the sum of the tunneling contributions $W_{\mu'\mu}^{tun}$ turns out to be smaller than the value obtained in the one-dimensional model. A simpler explanation of the slow-down may be given by considering the effective reduced mass of the transfer motion. Since the potential minima are tilted towards the nearest saddle points (see Fig. 3b), the transfer requires a cooperative q displacement near the minima, leading to an increase in the effective reduced mass to which the light H species is the most sensitive. In the D and T species, however, the relative increase in reduced mass is smaller and the enhancement of the tunnel interactions in excited q-mode states is sufficient to promote the transfer.

Model 6. Lowering the frequency of the coupled q mode to 109 cm^{-1} leads to an increase in effective reduced mass that is significant in all three species and therefore to a slow-down of hydrogen transfer that is only weakly dependent of isotopic mass. As in model 3, the capacity of the low frequency mode to activate the transfer appears to be exhausted at the experimental temperatures.

3.4 Modes Coupled by sinϕ and cosϕ

The ring framework modes of the types b_{2u} and b_{3u} in porphin [37] involve kite-shaped deformations of the arrangement of the four nitrogens. They occur in pairs (a,b) that are only slightly split in most cases. Examples are $\nu_{37\,a,b}$ at 1608, 1589, $\nu_{41\,a,b}$ at 1352, 1370, $\nu_{47\,a,b}$ at 949, 964, $\nu_{49\,a,b}$ at 345, 314, and $\nu_{50\,a,b}$ at 353, 353 cm^{-1}. In the limit of D_{4h} symmetry the pairs are degenerate and can then be related to two orthogonal trapezoidal deformations (see Fig. 3c) coupled to the transfer motion by the factors $\zeta(\phi)=\sin\phi$ and $\zeta(\phi)=\cos\phi$, respectively. We consider single modes at 1600 and at 960 cm^{-1} coupled by $\sin\phi$ in models 7 and 8, respectively, whereas we use an adiabatic approximation for a degenerate pair of modes at 340 cm^{-1} in model 9 that contains a coordinate q_s coupled by $\sin\phi$ and a coordinate q_c coupled by $\cos\phi$. The potential energy function, assumed as given by Eq. (9) and shown in Fig. 3c for the two-dimensional model, implies shifts in the (ϕ, q) plane and a lowering of the minima to a common depth from which the heights of the adjacent saddle points are measured to be approximately $B+2^{-1/2}\Delta V_{Rq}$ and $B-\Delta V_{Rq}(1-2^{-1/2})$. The potential energy function for model 9 is obtained by extending Eq. (9) to include the terms for both q_s and q_c.

From the results for models 3 and 6 we expect at low vibrational frequency a predominant effect by the q shifts that must occur when going from one minimum to the next. We therefore choose a simplified adiabatic approximation similar to that in Sect. 3.2. We use a product basis $\{\psi_\mu(\phi)\chi_{\mu vs}(q_s)\chi_{\mu vc}(q_c)\}$ where factors $\psi_\mu(\phi)$ of the transfer system refer to $q_s=q_c=0$ and are obtained as in the one-dimensional model. The factors $\chi_{\mu v}(q=\chi_v(q-q_{0\mu})$ are the harmonic oscillator functions centered at $q_{0\mu}=-\langle\mu|\zeta|\mu\rangle f_q/\omega_q^2$ with $\zeta=\sin\phi$ for $q=q_s$ and $\zeta=\cos\phi$ for $q=q_c$. In close analogy to Sect. 3.2, the tunneling contribution to a transition probability,

$$W_{\mu'\mu}^{tun} \propto [\Delta H_{\mu'\mu}]^2[\sum_{vs} p_{vs}^0 \langle\chi_{\mu' vs}|\chi_{\mu vs}\rangle^2][\sum_{vc} p_{vc}^0 \langle\chi_{\mu' vc}|\chi_{\mu vc}\rangle^2] \,, \tag{30}$$

is found to involve the product of the two mean square vibrational overlap factors. The same is true for the vibrational contribution.

Models 7–9. The behavior of the coupling effects is similar to that obtained from the models 1–3 (see Table 3) and may be explained similarly. The coupling of the transfer motion to a mode at 1600, 960, or 340 cm^{-1} results in a slow-down of transfer in the H species that levels off with increasing temperature except for the case of the low-frequency mode. The slow-down may be attributed to the larger effective mass being transferred. For the low-frequency mode at 340 cm^{-1}, this mass effect prevails with about equal efficiency in all three species and is practically constant in the experimental temperature range. For the 1600 and 960 cm^{-1} modes and the heavier D and T species the mass effect is less efficient and/or compensated by thermal activation through the new channels of transfer made available by the coupling.

3.5 Compatibility with Observation

The vibrational interaction effects collected in Table 3 are generally different for the three isotopic species and

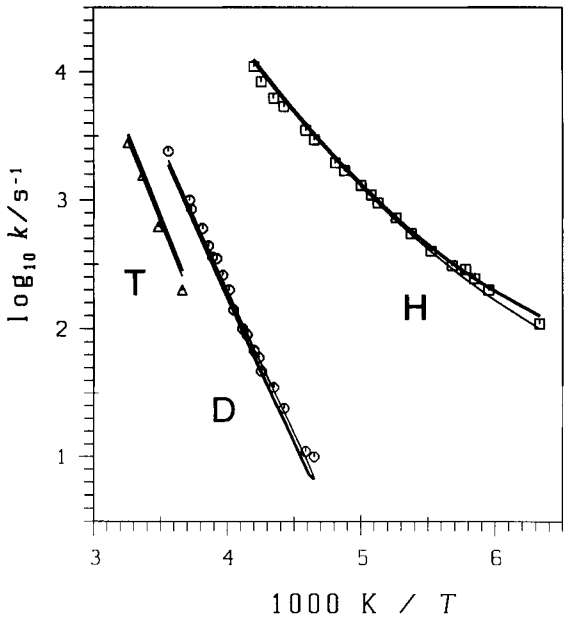

Fig. 5
Temperature dependence of the hydrogen transfer relaxation rate constant in the porphin anion. Squares, circles, and triangles indicate experimental data from Ref. [16] for H, D, and T species, respectively. The bold lines show the results calculated for a two-dimensional model involving a strong interaction with a rectangular displacement of the pyrrole rings, as suggested by the quantum chemical results of Ref. [38]. The thin lines show the one-dimensional model results

contradict the observed kinetic isotope effects if the q-mode frequency is near or above 960 cm^{-1}. In some cases, they also depend strongly on the temperature and therefore disagree with the observed slopes in the Arrhenius diagram. The largest discrepancies are found for the models 1, 2, 4, 5, 7, and 8, which involve vibrations at 960 cm^{-1} or at a higher frequency. Hence these models appear to be unrealistic and should therefore be rejected. This includes model 5 that mimics the behavior of the modes ν_{22} and δ_{NH} in porphin [37]. In the porphin anion, such a behavior contradicts the observations and is therefore unlikely to exist.

Coupling with a low frequency mode as in models 3, 6, and 9 leads to a slow-down that is similar for the three isotopic species and only weakly dependent on temperature. Such couplings could be compatible with experiment, provided that the slow-down effects are compensated by a suitable reduction of the barrier. One particular interaction, suggested by the quantum chemical results reported by Vangberg and Ghosh [38], involves a dominant rectangular displacement of the pyrrole rings, as in model 6 which involves a mode at 109 cm^{-1} (ν_{35} in porphin [37]). Using this type of model and its treatment in the adiabatic approximation (see Sect. 3.3), we have combined a large coupling with a reduced barrier near the predicted one [38] in a successful attempt to fit the temperature-dependent rate constants. The results are shown in Fig. 5. Although the standard deviation $\sigma(\ln k) = 0.19$ is somewhat larger than for the one-dimensional model, the predicted type of coupling [38] appears to be compatible with experiment. The model parameters are collected in Table 4. The barrier, i.e. the saddle point energy relative to the minima (see Fig. 3b for the qualitative behavior), is found at 4234 cm^{-1} (12.1 kcal/mol), close to the quantum chemical value of 11.8 kcal/mol [38]. The individual rearrangement energy ΔV_{Rq} found at 1475 cm^{-1} (4.2 kcal/mol) is much larger than the value of 200 cm^{-1} assumed for model 6 (see Table 3), and it indicates a very strong coupling. At $q = 0$ this yields a barrier of 5709 cm^{-1} and a frequency of 1168 cm^{-1} for the H vibration in the transfer direction. The remaining parameters are similar to those of the one-dimensional model except for a considerably smaller ΔV_a value which suggests easier delocalization of the highly excited states of the transfer mode.

Table 4
Parameters of a two-dimensional model for hydrogen transfer in the porphin anion

Parameter	Units	Value
B/hc_0	cm^{-1}	4233.8 (53)[a]
$\omega_q/2\pi c_0$	cm^{-1}	109.0[b]
$\Delta V_{Rq}/hc_0$	cm^{-1}	1475 (30)
$\omega_p/2\pi c_0$	cm^{-1}	21.3 (22)
$\Delta V_R/hc_0$	cm^{-1}	49.8 (19)
$\Delta V_a/hc_0$	cm^{-1}	9.21 (86)
$\Delta E_c/h$	MHz	105.5 (60)

[a]) Numbers in parentheses give standard deviations in units of last digit.
[b]) Fixed.

4. Summary and Conclusion

Using the master equation approach for the populations of localized quantum states of the transfer system, we have shown that the observed hydrogen transfer rate constants for the porphin anion can be reproduced by a one-dimensional model that describes a circular motion of the hydrogen atom in the plane of the porphin ring system. The model involves five parameters that are common to the H, D, and T isotopic species. The barrier of a fourfold symmetric potential energy function is obtained and predicts the in-plane N-H wagging mode in the expected frequency region. Two parameters describe the system-bath interaction in a simplified picture. They indicate a coupling that is most pronounced for low-frequency modes of the heat bath and that is moderate in overall strength. The remaining two parameters are related to the extent of localization of the basis states, a property found to be important when restricting the master equation to the populations. Not involving any promotion by a ring-framework mode, the model describes the system as 'self promoting' by direct excitation of the vibration of the hydrogen atom in the transfer direction.

Interaction effects of a variety of individual modes of the ring framework have been calculated and discussed in qualitative terms, invoking relative increases in effective

reduced mass and promotion by a framework mode. The interactions have been found to yield apparent activation energies and/or kinetic isotope effects that are incompatible with experiment unless the mode involved oscillates at low frequency. In particular, a behavior resembling that of the modes ν_{22} and δ_{NH} in porphin [37] is found to disagree with observations for the porphin anion. An interaction of the transfer motion with a rectangular displacement of the pyrrole rings, recently predicted from quantum chemistry [38], has been included in a two-dimensional model fitted to be experimental data. This model has been found to the compatible with the observations when assuming a low vibrational frequency, a lower barrier than in the one-dimensional system, and a massive coupling strength.

Since the observed data can be reproduced by either one of the two intrinsically different models, a serious gap in the presently available experimental information has become evident. In the two-dimensional model, complementary properties obtained from quantum chemistry are able to bridge this gap, but remain in need of experimental confirmation. When accepting the two-dimensional model as the more realistic one, the one-dimensional model must be considered as describing the transfer motion in the average over the many states of the strongly coupled vibration. The 'effective' one-dimensional model is still able to reproduce the observed kinetic isotope effects and correctly interprets the observed apparent activation energies as due to self promotion of the transfer.

Appendix

To calculate the transition probabilities, we extend the approach of Ref. [32] to a heat bath consisting of four parts that are coupled to the system by different factors $\zeta(\phi)$, as introduced in Sect. 2.3. We consider the "active bath displacements", $r_c=\sum_i f_{c,i}Q_{c,i}$, $r_s=\sum_i f_{s,i}Q_{s,i}$ etc. and assume equal power spectral density functions for each part,

$$J_{rr}(\omega)=\rho(\omega)f(\omega)^2\frac{h/2\pi}{\omega[\exp\{h\omega/2\pi k_B T\}-1]}\ , \tag{A1}$$

as given by the model function in Eq. (14). The frequency range of $J_{rr}(\omega)$ includes the negative values. In the numerical representation, the function is truncated at $|\omega|/2\pi c_0=4096\ \mathrm{cm}^{-1}$ and sampled at steps of $4\ \mathrm{cm}^{-1}$. All of the following operations are carried out numerically. The correlation function corresponding to $J_{rr}(\omega)$ is obtained by Fourier transformation,

$$C_{rr}(t)=(2\pi)^{-1}\int_{-\infty}^{\infty}\mathrm{d}\omega\ \mathrm{e}^{\mathrm{i}\omega t}J_{rr}(\omega)\ . \tag{A2}$$

Fourier transformation of the power spectral density function $J_{ss}(\omega)=\omega^{-2}J_{rr}(\omega)$ yields the correlation function of the "active bath momentum" [32],

$$C_{ss}(t)=(2\pi)^{-1}\int_{-\infty}^{\infty}\mathrm{d}\omega\,\mathrm{e}^{\mathrm{i}\omega t}\omega^{-2}J_{rr}(\omega)\ , \tag{A3}$$

that is used to account for bath oscillator shifts induced by the transfer motion.

The probability of a $\mu'\leftarrow\mu$ transition consists of a "tunneling" contribution due to the interaction element $\Delta H_{\mu'\mu}$ and "vibrational" contributions due to the elements $\zeta_{\mu'\mu}=\langle\mu'|\zeta(\phi)|\mu\rangle$ of the various coupling factors. It depends on the transition frequency

$$\omega_{\mu'\mu}=(2\pi/h)(E'_{\mu'}-E'_{\mu}) \tag{A4}$$

obtained from energy levels corrected by the rearrangement effects [32],

$$E'_\lambda=E_\lambda-\Delta V_R\{[(\cos\phi)_{\lambda\lambda}]^2+[(\sin\phi)_{\lambda\lambda}]^2]+[(\cos 2\phi)_{\lambda\lambda}]^2 + [(\sin 2\phi)_{\lambda\lambda}]^2\}\ , \tag{A5}$$

and is also sensitive to the squared distance of the two states in ζ space, in the present case given by

$$d^2_{\mu'\mu}=[(\cos\phi)_{\mu'\mu'}-(\cos\phi)_{\mu\mu}]^2+[(\cos 2\phi)_{\mu'\mu'}-(\cos 2\phi)_{\mu\mu}]^2 + [(\sin\phi)_{\mu'\mu'}-(\sin\phi)_{\mu\mu}]^2+[(\sin 2\phi)_{\mu'\mu'}-(\sin 2\phi)_{\mu\mu}]^2. \tag{A6}$$

The tunneling contribution is derived from the correlation function

$$C^{\mathrm{tun}}_{\mu'\mu}(t)=\exp\{d^2_{\mu'\mu}(2\pi/h)^2[C_{ss}(t)-C_{ss}(0)]\} \tag{A7}$$

and is proportional to its Fourier transform $J^{\mathrm{tun}}_{\mu'\mu}(\omega)$ sampled at the transition frequency $\omega=\omega_{\mu'\mu}$. As the function $J^{\mathrm{tun}}_{\mu'\mu}(\omega)$ diverges at $\omega=0$ we assume that transition frequencies may be arbitrarily small in magnitude but not exactly zero as a result of sufficiently long-lived perturbations expected to be present in condensed phase. Multiplication by the square of the tunnel interaction, expressed in angular frequency units, then yields the tunneling probability

$$W^{\mathrm{tun}}_{\mu'\mu}=(\Delta H_{\mu'\mu}2\pi/h)^2J^{\mathrm{tun}}_{\mu'\mu}(\omega_{\mu'\mu})\ . \tag{A8}$$

Similarly the vibrational contributions arise from the correlation function

$$C^{\mathrm{vib}}_{\mu'\mu}(t)=C_{rr}(t)C^{\mathrm{tun}}_{\mu'\mu}(t) \tag{A9}$$

and are given by the respective power spectral density $J^{\mathrm{vib}}_{\mu'\mu}(\omega_{\mu'\mu})$, multiplied by the sum of coupling factors $[\zeta_{\mu'\mu}2\pi/h]^2$,

$$W^{\mathrm{vib}}_{\mu'\mu}=\{[(\cos\phi)_{\mu'\mu}]^2+[(\sin\phi)_{\mu'\mu}]^2+[(\cos 2\phi)_{\mu'\mu}]^2 + [(\sin 2\phi)_{\mu'\mu}]^2\}(2\pi/h)^2J^{\mathrm{vib}}_{\mu'\mu}(\omega_{\mu'\mu})\ . \tag{A10}$$

The results of Eqs. (A8) and (A10) yield the total transition probability in Eq. (18).

We are grateful to the European Union for support of this work within the "Human Capital and Mobility" network "Localization and Transfer of Hydrogen" and to the ETH Zürich for a grant of free Cray J90 computer time for part of the computations. We also wish to thank Professors R.R. Ernst and J. Manz for many stimulating discussions.

References

[1] E.F. Caldin and V. Gold, Proton Transfer Reactions, Chapman and Hall, London 1975.
[2] F. Hibbert, Adv. Phys. Org. Chem. *22*, 113 (1986).
[3] R.P. Bell, The Proton in Chemistry, Chapman and Hall, London 1973.

[4] P.F. Barbara and H.P. Trommsdorff (Eds.), Spectroscopy and dynamics of elementary proton transfer in polyatomic systems, Chem. Phys. *136*, 153–360 (1989).
[5] R.P. Bell, The Tunnel Effect in Chemistry, Chapman and Hall, London 1980.
[6] V.A. Benderskii, V.I. Goldanskii, and J. Jortner (Eds.), Tunneling in Chemical Reactions, Chem. Phys. *170*, 265–460 (1993).
[7] P.F. Barbara, P.K. Walsh, and L.E. Brus, J. Phys. Chem. *93*, 29 (1989).
[8] J. Manz and L. Wöste (Eds.), Femtosecond Chemistry, Verlag Chemie, Weinheim and New York 1994.
[9] J.L. Herek, S. Pedersen, L. Bañares, and A.H. Zewail, J. Chem. Phys. *97*, 9046 (1992).
[10] J.A. Syage, J. Phys. Chem. *97*, 12523 (1993).
[11] T.J. Butenhoff and C.B. Moore, J. Am. Chem. Soc. *110*, 8336 (1988).
[12] H.H. Limbach, in: NMR – Basic Principles and Progress, Vol. 23, Chap. 2, ed. by P. Diehl, E. Fluck, H. Günther, R. Kosfeld, and J. Seelig, Springer, Berlin, 1990.
[13] a) A. Stöckli, B.H. Meier, R. Kreis, R. Meyer, and R.R. Ernst, J. Chem. Phys. *93*, 1502 (1990) and references cited therein; b) A. Heuer and U. Haeberlen, J. Chem. Phys. *95*, 4201 (1991); c) P. Robyr, B.H. Meier, and R.R. Ernst, Chem. Phys. Lett. *187*, 471 (1991); d) S. Takeda, A. Tsuzumitani, and C.A. Chatzidimitriou-Dreismann, Chem. Phys. Lett. *198*, 316 (1992); e) A.J. Horsewill, P.J. McDonald, and D. Vijayaraghavan, J. Chem. Phys. *100*, 1889 (1994); f) D.F. Brougham, A.J. Horsewill, and R.I. Jenkinson, Chem. Phys. Lett. *272*, 69 (1997).
[14] J. Braun, M. Schlabach, B. Wehrle, M. Köcher, E. Vogel, and H.H. Limbach, J. Am. Chem. Soc. *116*, 6593 (1994).
[15] J. Braun, Ch. Hasenfratz, R. Schwesinger, and H.H. Limbach, Angew. Chem. Int. Ed. Engl. *33*, 2215 (1994).
[16] J. Braun, R. Schwesinger, P.G. Williams, H. Morimoto, D.E. Wemmer, and H.H. Limbach, J. Am. Chem. Soc. *118*, 11101 (1996).
[17] W. Siebrand, T.A. Wildman, and M.Z. Zgierski, J. Am. Chem. Soc. *106*, 4083, 4089 (1984).
[18] Z. Smedarchina, W. Siebrand, and T.A. Wildman, Chem. Phys. Lett. *143*, 395 (1988); Z. Smedarchina, W. Siebrand, and F. Zerbetto, Chem. Phys. *136*, 285 (1989).
[19] Z.K. Smedarchina and W. Siebrand, Chem. Phys. *170*, 347 (1993).
[20] Z. Smedarchina, W. Siebrand, M.Z. Zgierski, and F. Zerbetto, J. Chem. Phys. *102*, 7024 (1995).
[21] A. Abragam, The Principles of Nuclear Magnetism, Clarendon, Oxford 1961.
[22] C.P. Slichter, Principles of Magnetic Resonance, Harper, New York 1964.
[23] A.G. Redfield, Adv. Magn. Reson. *1*, 1 (1965).
[24] K. Blum, Density Matrix Theory and Applications, Plenum Press, New York and London 1981.
[25] R. Wertheimer and R. Silbey, Chem. Phys. Lett. *75*, 243 (1980).
[26] V. Romero-Rochin and I. Oppenheim, Physica A *155*, 52 (1989); V. Romero-Rochin, A. Orsky, and I. Oppenheim, Physica A *156*, 244 (1989).
[27] L. Vodná, J. Chem. Phys. *94*, 6553 (1991).
[28] R. Silbey and R.A. Harris, J. Phys. Chem. *93*, 7062 (1989).
[29] A.J. Leggett, S. Chakravarty, A.T. Dorsey, M.P.A. Fisher, A. Garg, and W. Zwerger, Rev. Mod. Phys. *59*, 1 (1987).
[30] A. Suárez and R. Silbey, J. Chem. Phys. *94*, 4809 (1991); Heuer, Ref. [13b] 1991.
[31] P.E. Parris and R. Silbey, J. Chem. Phys. *83*, 5619 (1985).
[32] R. Meyer and R.R. Ernst, J. Chem. Phys. *93*, 5518 (1990).
[33] R. Meyer, J. Chem. Phys. *52*, 2053 (1970); J. Mol. Spectrosc. *76*, 266 (1979). This method uses a discrete variable representation that is strictly equivalent to the variational representation in a basis of trigonometric functions. It yields the energy levels of 1D and 2D systems with sufficient accuracy to allow one to calculate even small tunnel splittings as differences of relatively large calculated energy levels. The results were converged within 0.01 MHz for all three isotopic species when resolving the range $-\pi<\phi\leq\pi$ into 89 grid points.
[34] B.M.L. Chen and A. Tulinsky, J. Am. Chem. Soc. *94*, 4144 (1972); A. Tulinsky, Ann. N.Y. Acad. Sci. *206*, 47 (1973).
[35] O. Brackhagen, O. Kühn, J. Manz, V. May, and R. Meyer, J. Chem. Phys. *100*, 9007 (1994); see also V. May, O. Kühn, and M. Schreiber, J. Phys. Chem. *97*, 12591 (1993).
[36] O. Brackhagen, Dissertation, Freie Universität Berlin, 1994.
[37] X.-Y. Li and M.Z. Zgierski, J. Phys. Chem. *95*, 4268 (1991).
[38] T. Vangberg and A. Ghosh, J. Phys. Chem. B *101*, 1496 (1997).
[39] L. Nygaard, J.T. Nielsen, J. Kirchheiner, G. Maltesen, J. Rastrup-Andersen, and G.O. Sorensen, J. Mol. Struct. *42*, 491 (1969).
[40] Ch. Scheurer and P. Saalfrank, Chem. Phys. Lett. *245*, 201 (1995); J. Chem. Phys. *104*, 2869 (1996).
[41] D.C. Look and I.J. Lowe, J. Chem. Phys. *44*, 2995 (1966); *44*, 3437 (1966).

Presented at the Discussion Meeting of the Deutsche Bunsen-Gesellschaft für Physikalische Chemie “Hydrogen Transfer: Experiment and Theory” in Berlin, September 10th to 13th, 1997 E 9759